Chinese Materials Research Society

Progress in Natural Science: Materials International

ORIGINAL RESEARCH

Hybrid brominated sulfonated poly(2,6-diphenyl-1,4-phenylene oxide) and SiO_2 nanocomposite membranes for CO_2/N_2 separation

Bing Yu[a,b], Hailin Cong[a,b,*], Xiusong Zhao[b,c]

[a]College of Chemical and Environmental Engineering, Qingdao University, Qingdao 266071, China
[b]Laboratory for New Fiber Materials and Modern Textile, Growing Base for State Key Laboratory, Qingdao University, China
[c]The University of Queensland, School of Chemical Engineering, Brisbane, QLD 4072, Australia

Abstract Brominated sulfonated poly(2,6-diphenyl-1,4-phenylene oxide) ($BSPPO_{dp}$) was synthesized as a new membrane material for CO_2/N_2 separation. The 90% brominated-10% sulfonated PPO_{dp} ($BSPPO_{dp}9010$) was selected as representative material for membrane preparation. It formed flexible membranes with higher CO_2 permeability ($P_{CO_2}=58$ Barrer) and selectivity ($\alpha_{CO_2/N_2}=36$) than poly(2,6-dimethyl-1,4-phenylene oxide) (PPO_{dm}) membranes. $BSPPO_{dp}9010$ membranes containing silica nanoparticles enhanced CO_2 permeability while maintaining the CO_2/N_2 selectivity as compared with the pure $BSPPO_{dp}9010$ membranes. The CO_2 permeability increased as a function of the silica content in the membrane. The separation mechanism for CO_2/N_2 in the membranes was attributed to the gas solubility effect rather than the gas diffusivity.

*Corresponding author at: College of Chemical and Environmental Engineering, Qingdao University, Qingdao 266071, China.
Tel.: +86 532 85083445; fax: +86 532 85955529.
E-mail address: hailincong@yahoo.com (H. Cong).

1. Introduction

Global warming resulting from the increased CO_2 concentration in the atmosphere from fossil fuel combustion is becoming one of the most important environmental global issues [1–3]. Thus the efficient and economical separation of CO_2 from N_2 in flue gases are receiving significant attention from the industry and government around the world [4,5]. Polymer-based gas separation membranes are inexpensive, less energy intensive requiring no phase change in the process, and have been used in industrial applications including the production of high purity N_2, gas dehydration, and recovery hydrogen from process streams [6–8].

Poly(2,6-dimethyl-1,4-phenylene oxide) (PPO_{dm}) as a membrane material for gas separation has been well reported [9,10]. The unique property drawing the attention of many researchers is its high gas permeation, particularly CO_2. At room temperature, the CO_2 permeability of the PPO_{dm} membrane is higher than 40 Barrer, and the selectivity is about 15 for CO_2/N_2, which is superior to other glassy polymers like polysulfone and polycarbonates [11–14]. It is worth to mention that in this paper the selectivity means permselectivity obtained from pure gas permeation tests unless indicated elsewhere. Chemical modification has been used to further improve the gas separation performance of these membranes. Story et al. [15] reported that introducing bromine groups into the aromatic ring position of PPO_{dm} further increased the CO_2 permeability by 2.5 times without sacrificing the selectivity over CH_4. In contrast, introducing bromines to the methyl groups of PPO_{dm} substantially decreased both the permeability and selectivity. Hamad et al. [16] further improved the CO_2 selectivity over CH_4 by introducing a certain amount of sulfonic acid groups to the brominated PPO_{dm} ($BPPO_{dm}$) at ring position. However, it is generally difficult to chemically modify polymers to improve both permeability and selectivity due to the tradeoff between permeability and selectivity [17,18]. For instance, compared to PPO_{dm}, the pyridinium-based ionic liquid modified PPO_{dm} (PyIPPO) had increased CO_2/N_2 selectivity (α_{CO_2/N_2}) but decreased CO_2 permeability (P_{CO_2}) [19].

Another route to enhance the gas separation performance of polymer membrane is by impregnating the polymeric matrix with nanoparticles (NPs) [20–26]. Recent studies have shown that such nanocomposite membranes have substantially increased permeability without deteriorating the selectivity [27–30]. Specifically, silica NPs were found by Merkel et al. [31] to be especially effective in increasing the gas permeability of poly(4-methyl-2-pentyne) (PMP) membranes, for example, 30 wt % silica NPs doubled the n-butane/methane selectivity and increased the n-butane permeability by a factor of 3 relative to pure PMP. The hybrid membranes of poly(amide-6-b-ethylene oxide) (PEBAX) and silica (27 wt%) had a P_{CO_2} of 277 Barrer and a α_{CO_2/N_2} of 79 [32]. The nanocomposite membranes that contained 0.3 weight ratio of silica/$BPPO_{dm}$ had a P_{CO_2} of 523 Barrer and a α_{CO_2/N_2} of 21 [33].

In this paper, we proposed that PPO with more bulky groups might have higher gas permeability than the PPO_{dm}-based membrane. We thus synthesized poly(2,6-diphenyl-1,4-phenylene oxide) (PPO_{dp}), brominated PPO_{dp} ($BPPO_{dp}$), and brominated sulfonated PPO_{dp} ($BSPPO_{dp}$) as derivates of PPO, and investigated theirs membrane performance. PPO_{dp} membranes had low gas permeability due to crystallization of the polymer chains. Both $BPPO_{dp}$ and $BSPPO_{dp}$ membranes had higher CO_2 permeability than PPO_{dm}, and the $BSPPO_{dp}$ membranes had a higher CO_2/N_2 selectivity than $BPPO_{dp}$. Therefore, the nanocomposite membranes of $BSPPO_{dp}$ and silica NPs were studied to further improve the CO_2 permeability without sacrificing the high CO_2 selectivity over N_2. The effect of composition as well as the separation mechanism of the membranes were investigated and discussed accordingly.

2. Experimental section

2.1. Chemicals

PPO_{dm} (Mn~25,000, polydispersity~2.0), 2,6-diphenylphenol (98%), N,N,N',N'-tetramethylethylenediamine (TMEDA, 99%),

bromine (Br_2, 99.5%), chloroform ($CHCl_3$, 99.8%), methanol (99.8%), ethanol (99.5%), 1,2-dichlorobenzene (99%), anhydrous hydrazine (98%), anhydrous magnesium sulfate (99.5%), chlorosulfonic acid (99%), glacial acetic acid (99.7%) and 10 nm silica nanopowders (SiO_2, 99.5%) were purchased from Aldrich and used as received. Copper(I) chloride (CuCl, 93.2%) from J. T. Baker Chemical Co. was stirred with glacial acetic acid, filtered, washed with ethanol and dried.

2.2. Synthesis of PPO_{dp}

PPO_{dp} was synthesized according to the method reported by Hay [34]. A typical procedure is as the follows: 0.041 g of CuCl, 0.031 g of TMEDA, 2 g of anhydrous magnesium sulfate and 35 ml of 1,2-dichlorobenzene were added to a 100 ml flask. The flask was heated in an oil bath at 65 °C and the mixture was agitated with a magnetic stirrer. Oxygen was bubbled through the mixture for 10 min. When the solution became green colored, a solution of 5 g of 2,6-diphenylphenol in 40 ml of 1,2-dichlorobenzene was added slowly over 20 min. A dark red color developed instantly. The reaction continued for 24 h. When the reaction was finished, several drops of anhydrous hydrazine were added into the reaction mixture to reduce the diphenoquinone byproducts. The inorganic solids were removed by filtration and the solution was added dropwise to 400 ml of methanol containing several drops of hydrazine. After stirring for several hours, the polymer was collected by filtration. The polymer was redissolved in 40 ml of chloroform and precipitated in 400 ml of methanol. The polymer (3 g) with Mn~150,000 was collected by filtration and dried in a vacuum oven at 80 °C for 24 h.

2.3. Synthesis of $BSPPO_{dp}$

An amount of 5 g PPO_{dp} and 50 ml of $CHCl_3$ were added to a 100 ml flask. The mixture was agitated with a magnetic stirrer. A solution of 8–10 ml of bromine diluted with 10 ml of chloroform was added dropwise to the mixture over a 30 min period. The mixture maintained a dark red color throughout the bromination reaction. Argon was bubbled into the solution to remove the HBr formed in the reaction. After stirring at room temperature for 1 h, the polymer was precipitated out in 800 ml of mechanically stirred ethanol. The polymer was filtered and dried under vacuum at room temperature. The extent of bromination was 80–100% from NMR spectrum. Brominated PPO_{dp} at 80–90% of bromination was further reacted with stoichiometric amount of chlorosulfonic acid under nitrogen atmosphere following the general procedure described in detail elsewhere [35]. The extent of sulfonation for the brominated PPO_{dp} was 10–20% from NMR spectrum.

2.4. Membrane preparation

The 80% brominated-20% sulfonated PPO_{dp} ($BSPPO_{dp}8020$), 90% brominated-10% sulfonated PPO_{dp} ($BSPPO_{dp}9010$), 100% brominated PPO_{dp} ($BPPO_{dp}$), PPO_{dm} and PPO_{dp} were selected as representative materials for membrane preparation. PPO_{dm}, PPO_{dp}, $BPPO_{dp}$ and $BSPPO_{dp}$ membranes were cast on a glass plates at room temperature from their 3 wt% solutions of chloroform. The preparation of polymer/silica

membranes is as follows: the polymer (BSPPO$_{dp}$ 0.3 g) was dissolved in 5 ml of chloroform by stirring in a beaker. Silica NPs (10 nm) were added slowly to the polymer solution at 9.9, 20.5, and 29.9 wt% of the polymer, respectively. The mixture was vigorously stirred at a rotation speed of 1150 rpm for 15 min in order for the nanoparticles to be dispersed uniformly in the polymer matrix. The mixture was then cast onto a clean Rain·X treated glass plate at room temperature and left open to atmosphere. After the solvent was evaporated, the resulting membrane was peeled off and stored in a desiccator for testing. The thickness of the membrane was about 50–90 μm.

2.5. Characterization

PPO$_{dm}$, PPO$_{dp}$, BPPO$_{dp}$ and BSPPO$_{dp}$ samples were dissolved in deuterated chloroform at a concentration of $\sim$2% by weight for ^{1}H-NMR analyses on a Bruker Advance DRX-400 spectrometer. Glass transition temperature (T_g) were determined by a differential scanning calorimeter (TA Instruments, model QP10). The heating rate was 20 °C/min. All tests were repeated at least twice to ensure the reproducibility. Scanning electron microscope (SEM) (Philips 505) and transmission electron microscope (TEM) (Hitachi H-7000) were used to observe the morphology and dispersion of particles in the membranes. The operation voltage of SEM was 10 kV.

2.6. Gas separation performance test

The pure gas permeability was measured in a constant-volume variable-pressure unit similar to those described in [36–38] and schematically shown in Fig. 1. The diffusion cell was divided into an upstream side and a downstream side by a membrane.
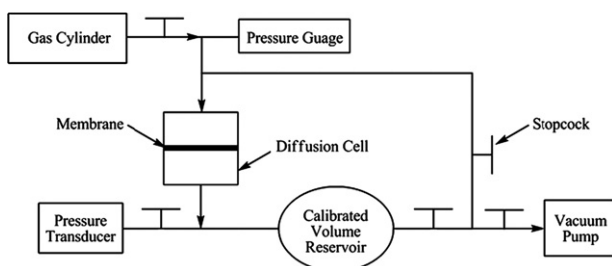

Fig. 1 Schematic illustration of the constant-volume variable-pressure permeation test setup.

The downstream side volume was calibrated and its pressure was monitored by a pressure transducer. The membrane area was 46.5 cm^2. Before conducting a measurement, the entire system was evacuated to about 10 Pa. Then the gas was charged from a cylinder to the cell upstream side and kept at a constant pressure of 6.88×10^4 Pa (10 psig). The value of gas permeability measured was determined from

$$P = \frac{VL}{ART\Delta P}\left[\left(\frac{dp}{dt}\right)HP - \left(\frac{dp}{dt}\right)LP\right] \tag{1}$$

where P is the permeability (cm^3(STP) cm/cm^2 s cm Hg), V is the downstream volume (cm^3), L is the membrane thickness (cm), A is the membrane area (cm^2), R is the gas constant ($=0.278$ cmHg cm^3/cm^3(STP) K), T is the absolute temperature (K), ΔP is the transmembrane pressure difference ($=p_2 - p_1$, where p_2 and p_1 are the upstream and downstream pressures (cm Hg), respectively), and $(dp/dt)_{HP}$ and $(dp/dt)_{LP}$ are the steady-state rates of pressure rise (cm Hg/s) in the downstream volume at a fixed high upstream pressure and under low vacuum pressure, respectively [39]. The diffusivity (D) was determined from

$$D = L^2/6\theta \tag{2}$$

where θ is the time lag when a steady dp/dt rate is obtained on the downstream side in the permeation tests [40]. The solubility (S) was determined from

$$S = P/D \tag{3}$$

and the permselectivity (α) was determined from

$$\alpha = P_A/P_B \tag{4}$$

where P_A and P_B are the permeabilities of pure gases A and B, respectively.

Table 1 DSC testing results of PPO derivatives.

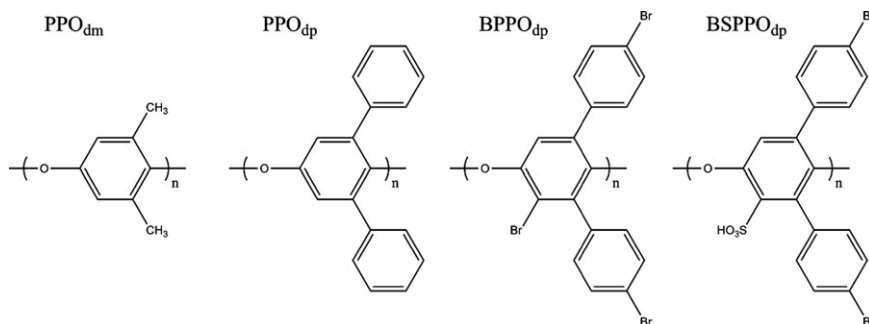| Sample	T_g (°C)	T_m (°C)
PPO$_{dm}$	216	–
PPO$_{dp}$	235	470
BPPO$_{dp}$	288	–
BSPPO$_{dp}$9010	284	–
BSPPO$_{dp}$8020	281	–

Fig. 2 PPO derivates used in this study.

Table 2 Gas separation performance of polymer membranes of PPO derivatives.

Polymer membranes	P_{CO_2} (Barrer)	P_{N_2} (Barrer)	α_{CO_2/N_2}	$D_{CO_2} \times 10^8$ (cm^2/s)	S_{CO_2} (cm^3(STP)/cm^3 cm Hg)
PPO$_{dm}$	48.4	3.3	14.7	7.4	7.2
PPO$_{dp}$	24.5	1.6	15.3	5.1	5.5
BPPO$_{dp}$	78.0	2.6	30.0	8.7	9.8
BSPPO$_{dp}$9010	57.7	1.6	36.1	5.8	10.9
BSPPO$_{dp}$8020	48.0	1.2	40.0	4.5	11.7

Test condition: 10 psig feed pressure and room temperature.

3. Results and discussion

3.1. Characterization of PPO derivates and their membranes

A schematic representation of the PPO derivatives used for this study is shown in Fig. 2. The PPO$_{dm}$ and PPO$_{dp}$ are white powders, while the BPPO$_{dp}$ and BSPPO$_{dp}$ are yellowish powders. The DSC results of PPO$_{dm}$, PPO$_{dp}$, BPPO$_{dp}$ and BSPPO$_{dp}$ are listed in Table 1. The T_g's of PPO$_{dm}$, PPO$_{dp}$, BPPO$_{dp}$, BSPPO$_{dp}$9010 and BSPPO$_{dp}$8020 are 216 °C, 235 °C, 288 °C, 284 °C and 281 °C, respectively. The bulky phenyl side chains in each repeat unit of PPO$_{dp}$ decrease the flexibility of the polymer chain, and thus PPO$_{dp}$ has a higher T_g than PPO$_{dm}$. For BPPO$_{dp}$ and BSPPO$_{dp}$, the bulky bromine/sulfonic groups in the phenyl side chains and the backbone further increase their T_g properties. The results in Table 1 indicate that PPO$_{dp}$ is crystallized with a melting point (T_m) at 470 °C. In contrast, PPO$_{dm}$, BPPO$_{dp}$ and BSPPO$_{dp}$ remain amorphous.

PPO$_{dm}$, PPO$_{dp}$, BPPO$_{dp}$ and BSPPO$_{dp}$ form very good membranes on glass plates at room temperature from their 3 wt% solutions. The gas separation results of the five polymer membranes are displayed in Table 2. The BSPPO$_{dp}$9010 membrane has a P_{CO_2} of 58 Barrer and α_{CO_2/N_2} of 36. Both are better than those of the PPO$_{dm}$ membrane ($P_{CO_2} = 48.4$ Barrer, $\alpha_{CO_2/N_2} = 14.7$). The PPO$_{dp}$ membrane has a lower P_{CO_2} (24.5 Barrer) and α_{CO_2/N_2} (15.3) than PPO$_{dm}$ due to

crystallization. BPPO$_{dp}$ has the highest CO$_2$ permeability, while BSPPO$_{dp}$ has the highest CO$_2$/N$_2$ selectivity in the five materials. Further analysis clearly indicates that the increase in CO$_2$/N$_2$ selectivity is a result of the high CO$_2$ solubility (S_{CO_2}) in BSPPO$_{dp}$ membrane. Compared with BPPO$_{dp}$, BSPPO$_{dp}$9010 has a higher CO$_2$/N$_2$ selectivity. Compared with BSPPO$_{dp}$8020, BSPPO$_{dp}$9010 has a higher CO$_2$ permeability. Therefore, BSPPO$_{dp}$9010 is selected as representative material for nanocomposite membrane preparation.

3.2. Nanocomposite membranes and their gas separation performance

BSPPO$_{dp}$9010/silica nanocomposite membranes were prepared by mixing the polymers with 10 nm silica NPs in chloroform solutions. The obtained BSPPO$_{dp}$9010/silica membranes remained flexible up to 23 wt% silica in the composites. The SEM micrographs in Fig. 3 show the morphology of the BSPPO$_{dp}$9010/silica membranes. It is observed that silica NPs aggregate together to form clusters in the composite membranes; the number of clusters increases with the increase of the silica content. The TEM micrographs in Fig. 4 provide further information of the BSPPO$_{dp}$9010/silica membranes morphology. In some regions silica NPs aggregate together to form clusters (black parts), which is in accordance with the SEM images. In the region with no clusters (white parts), silica NPs disperse well in the polymer observed from the higher resolution TEM image.

The gas separation properties of BSPPO$_{dp}$9010/silica membranes with three silica concentrations (9, 17, and 23 wt%) are further tested for gas permeation. The permeability and selectivity (permselectivity) of the BSPPO$_{dp}$9010/silica membranes as a function of the silica weight percentage are summarized in Fig. 5. The permeabilities of CO$_2$ and N$_2$ increase with increasing
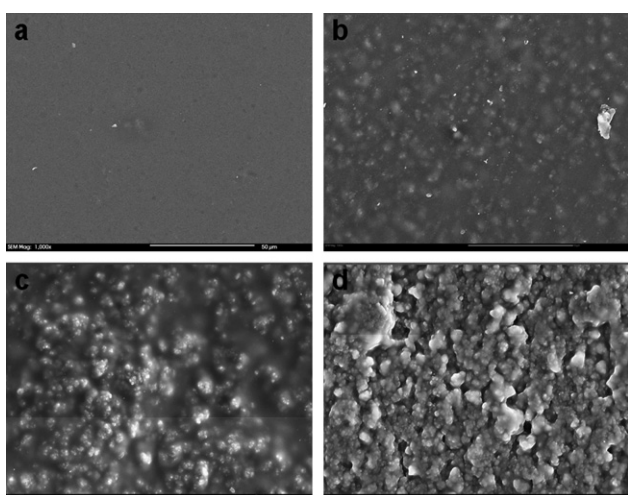

Fig. 3 SEM morphology of the BSPPO$_{dp}$9010/silica nanocomposite membranes at the silica content of (a) 0, (b) 9, (c) 17, and (d) 23 wt%. (Scale bar: 50 μm).
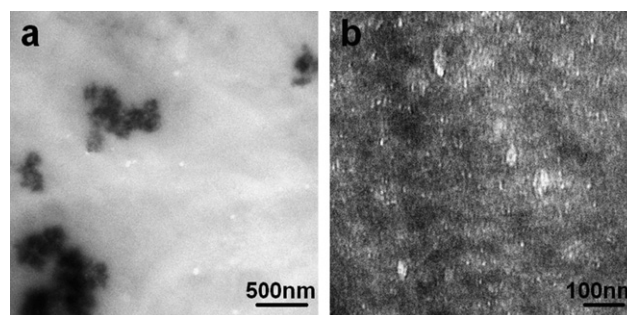

Fig. 4 TEM morphology of the BSPPO$_{dp}$9010/9 wt% silica nanocomposite membranes.
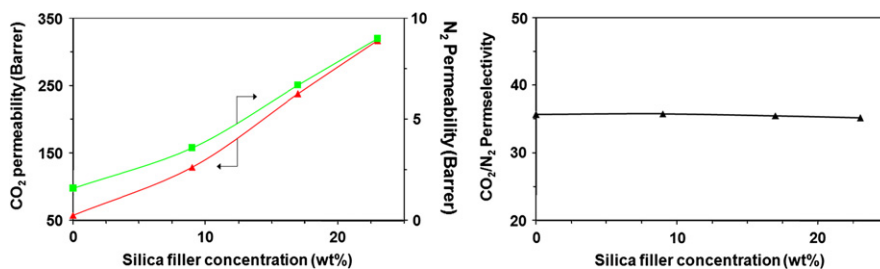
Fig. 5 Gas permeability and permselectivity of the $BSPPO_{dp}9010$/silica nanocomposite membrane as a function of the silica concentration. (Test condition: 10 psig feed pressure and room temperature).

Table 3 Gas separation performance of $BSPPO_{dp}9010$/9 wt% silica membranes fabricated from different polymer concentrations.

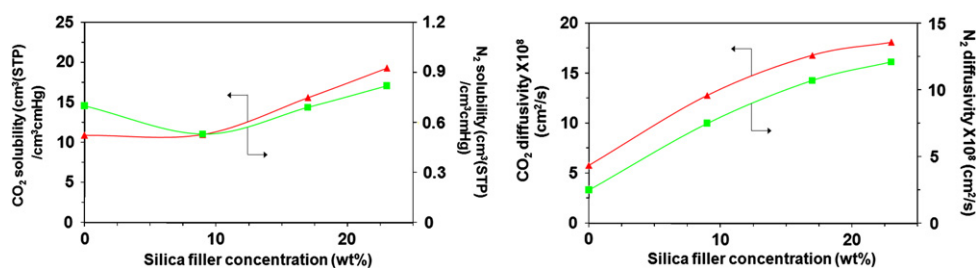| $BSPPO_{dp}9010$/9 wt% silica nanocomposite membranes	P_{CO_2} (Barrer)	P_{N_2} (Barrer)	α_{CO_2/N_2}
From 3.8 wt% polymer concentration	129	3.6	35.8
From 16 wt% polymer concentration	130	3.6	36.1

Fig. 6 Gas solubility and diffusivity in the $BSPPO_{dp}9010$/silica nanocomposite membrane as a function of the silica concentration. (Test condition: 10 psig feed pressure and room temperature).
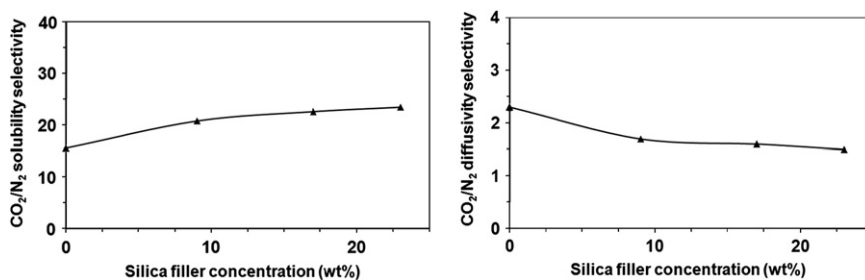

Fig. 7 CO_2/N_2 solubility and diffusivity ratios in the $BSPPO_{dp}9010$/silica nanocomposite membrane.

silica concentration. The P_{CO_2} of the $BSPPO_{dp}9010$/silica membrane is 129 Barrer at 9 wt% of silica, and reaches 317 Barrer at 23 wt% silica, about 5.5 times of that of the pure $BSPPO_{dp}9010$ membrane, while the CO_2/N_2 permselectivities in $BSPPO_{dp}9010$/silica membranes remain almost the same as pure $BSPPO_{dp}9010$ membranes, suggesting that silica NPs added to $BSPPO_{dp}9010$ polymer do not deteriorate the gas selectivity but can enhance the gas permeability.

Heterogeneity, which is defined as fillers separating out from the membrane matrix due to the gravity or incompatibility and forming separate filler phases or layers during the formation of the composite membranes, may occur in polymer–inorganic composite membranes. Heterogeneity may deteriorate the gas separation performance of the membranes. To test the possible heterogeneity of silica NPs in the membranes, two $BSPPO_{dp}9010$/9 wt% silica nanocomposite membranes are cast from 3.8 wt% and 16 wt% polymer solutions at the same filler-to-polymer ratio. The viscosity of the 16 wt% polymer solution is much higher than that of the 3.8 wt% solution and thus will minimize or inhibit heterogeneity of the silica NPs in the membranes. The results shown in Table 3 clearly indicate that the gas separation
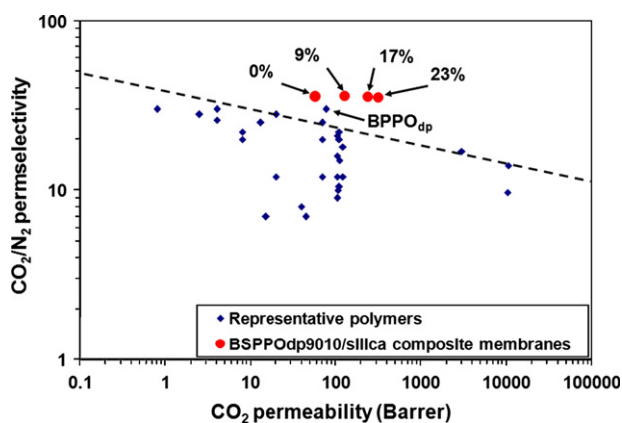
Fig. 8 Separation performance of the $BSPPO_{dp}9010/10$ nm-silica nanocomposite membranes at different silica concentrations.

performances of the two membranes have no difference, indicating that silica NPs do not undergo heterogeneity during the membrane casting.

The gas permeability of a membrane is proportional to diffusivity and solubility ($P=DS$). Thus, the diffusivity and solubility of the gases in the composite membranes are further analyzed. With increasing the silica concentration, solubilities of CO_2 and N_2 increase slightly, but the diffusivities of them increase considerably (Fig. 6). The increased gas diffusivity by adding nanoparticles into glassy polymer membranes may result in polymer chain packing re-arrangement resulting in increased free volume as reported elsewhere [31,32].

As shown in Fig. 7, the separation mechanism for CO_2/N_2 is primarily caused by the gas solubility difference rather than the gas diffusivity difference because the former ($\sim$20) is much larger than the latter ($\sim$1.5).

The $BSPPO_{dp}9010$/silica nanocomposite membranes have better gas separation performance than pure $BSPPO_{dp}9010$ and $BPPO_{dp}$ membranes. The pure $BSPPO_{dp}9010$ membrane has CO_2/N_2 separation performance above the Robeson's line [17] and moves towards the desirable upper right quadrant as the content of nanoparticles increases (Fig. 8). This indicates that $BSPPO_{dp}9010$/silica membranes may be useful for CO_2/ N_2 separation.

4. Conclusions

$BSPPO_{dp}9010$ is synthesized as a derivative of PPO. Compared with PPO_{dm} membranes, the CO_2 permeability and CO_2/N_2 permselectivity of the $BSPPO_{dp}9010$ membranes increase by 1.2 and 2.5 times, respectively. Silica particles with diameters of 10 nm are mixed with $BSPPO_{dp}9010$ at 9, 17, and 23 wt% to form $BSPPO_{dp}9010$/silica nanocomposite membranes. These hybrid membranes have greatly enhanced CO_2 permeability while maintaining the CO_2/N_2 selectivity compared to pure $BSPPO_{dp}9010$ membranes. The CO_2 permeability increases with the silica content in the membranes. The $BSPPO_{dp}9010/23$ wt% silica membrane has a higher performance delivering CO_2 permeability of 317 Barrer at room temperature with a CO_2/N_2 selectivity of 35.2. The separation mechanism for CO_2/N_2 in the membranes is primarily controlled by the gas solubility difference rather than the gas diffusivity difference.

References

[1] Z. Ma, Z. Xu, J. Zhou, Effect of global warming on the distribution of Lucifer intermedius and L. hanseni (Decapoda) in the Changjiang estuary, Progress in Natural Science 19 (2009) 1389.

[2] D. Shangguan, S. Liu, Y. Ding, L. Ding, J. Xu, L. Jing, Glacier changes during the last forty years in the Tarim interior river basin, northwest China, Progress in Natural Science 19 (2009) 727.

[3] Y. Zhu, S. Shang, W. Zhai, M. Dai, Satellite-derived surface water pCO_2 and air-sea CO_2 fluexs in the northern south China sea in summer, Progress in Natural Science 19 (2009) 775.

[4] B. Yu, H. Cong, X.S. Zhao, Z. Chen, Carbon dioxide capture by dendrimer-modified silica nanoparticles, Adsorption Science and Technology 29 (2011) 781.

[5] X. Ren, J. Ren, M. Deng, Poly(amide-6-b-ethylene oxide) membranes for sour gas separation, Separation and Purification Technology 89 (2012) 1.

[6] H. Lin, E.V. Wagner, B.D. Freeman, L.D. Toy, R.P. Gupta, Plasticization-enhanced hydrogen purification using polymeric membranes, Science 311 (2006) 639.

[7] W.J. Koros, R. Mahajan, Pushing the limits on possibilities for large scale gas separation: which strategies, Journal of Membrane Science 175 (2000) 181.

[8] H. Cong, M. Radosz, B.F. Towler, Y. Shen, Polymer–inorganic nanocomposite membranes for gas separation, Separation and Purification Technology 55 (2007) 281.

[9] G. Chowdhury, R. Vujosevic, T. Matsuura, B. Laverty, Effects of polymer molecular weight and chemical modification on the gas transport properties of poly(2,6-dimethyl-1,4-phenylene oxide), Journal of Applied Polymer Science 77 (2000) 1137.

[10] F. Hamad, K.C. Khulbe, T. Matsuura, Comparison of gas separation performance and morphology of homogeneous and composite PPO membranes, Journal of Membrane Science 256 (2005) 29.

[11] S. Sridhar, B. Smitha, M. Ramakrishna, T.M. Aminabhavi, Modified poly(phenylene oxide) membranes for the separation of carbon dioxide from methane, Journal of Membrane Science 280 (2006) 202.

[12] R.T. Chern, F.R. Sheu, L. Jia, V.T. Stannet, H.B. Hopfenberg, Transport of gases in unmodified and aryl-modified poly(2,6-dimethyl-1,4-phenylene oxide), Journal of Membrane Science 35 (1987) 103.

[13] G.A. Polotskaya, S.A. Agranova, T.A. Antonova, G.K. Elyashevich, Gas transport and structural features of sulfonated poly(phenylene oxide), Journal of Applied Polymer Science 66 (1997) 1439.

[14] G. Chowdhury, B. Kruczek, T. Matsuura, Polyphenylene Oxide and Modified Polyphenylene Oxide Membranes: Gas, Vapor, and

Liquid Separation, Kluwer Academic Publishers, Norwell, USA, 2001.

[15] B.J. Story, W.J. Koros, Sorption and transport of CO_2 and CH_4 in chemically modified poly(phenylene oxide), Journal of Membrane Science 67 (1992) 191.

[16] F. Hamad, T. Matsuura, Performance of gas separation membranes made from sulfonated brominated high molecular weight poly(2,4-dimethyl-l,6-phenyIene oxide), Journal of Membrane Science 253 (2005) 183.

[17] L.M. Robeson, Correction of separation factor versus permeability for polymeric membranes, Journal of Membrane Science 62 (1991) 165.

[18] G. Maier, Gas separation with polymer membranes, Angewandte Chemie International Edition 37 (1998) 2960.

[19] H. Cong, B. Yu, J. Tang, X.S. Zhao, Ionic liquid modified poly(2,6-dimethyl-1,4-phenylene oxide) for CO_2 separation, Journal of Polymer Research 19 (2012) 9761.

[20] R. Stephen, C. Ranganathaiah, S. Varghese, K. Joseph, S. Thomas, Gas transport through nano and micro composites of natural rubber (NR) and their blends with carboxylated styrene butadiene rubber (XSBR) latex membranes, Polymer 47 (2006) 858.

[21] R.D. Noble, R. Agrawal, Separations research needs for the 21st century, Industrial and Engineering Chemistry Research 44 (2005) 2887.

[22] T. Suzuki, Y. Yamada, Characterization of 6FDA-based hyperbranched and linear polyimide-silica hybrid membranes by gas permeation and ^{129}Xe NMR measurements, Journal of Polymer Science B 44 (2006) 291.

[23] P. Winberg, K. DeSitter, C. Dotremont, S. Mullens, I.F.J. Vankelecom, F.H. Maurer, Free volume and interstitial mesopores in silica filled poly(1-trimethylsilyl-1-propyen) nanocomposites, Macromolecules 38 (2005) 3776.

[24] H. Cong, X. Hu, M. Radosz, Y. Shen, Brominated poly(2,6-diphenyl-1,4-phenylene oxide) and its silica nanocomposite membranes for gas separation, Industrial and Engineering Chemistry Research 46 (2007) 2567.

[25] N.P. Patel, A.C. Miller, R.J. Spontak, Highly CO_2-permeable and selective polymer nanocomposite membranes, Advanced Materials 15 (2003) 729.

[26] H. Bai, X. Wang, Y. Zhou, L. Zhang, Preparation and characterization of poly(vinylidene fluoride) composite membranes blended with nano-crystalline cellulose, Progress in Natural Science: Materials International 22 (2012) 250.

[27] C. Joly, S. Goizet, J.C. Schrotter, J. Sanchez, M. Escoubes, Sol–gel polyimide–silica composite membrane: gas transport properties, Journal of Membrane Science 130 (1997) 63.

[28] D. Shekhawat, D.R. Luebke, H.W. Pennline, A Review of Carbon Dioxide Selective Membranes, U.S. Deparment of Energy, Morgantown, USA, 2003.

[29] Z. He, I. Pinnau, A. Morisato, Nanostructured poly(4-methy-2-pentyne)/silica hybrid membranes for gas separation, Desalination 146 (2002) 11.

[30] H. Cong, J. Zhang, M. Radosz, Y. Shen, Carbon nanotube composite membranes of brominated poly(2,6-diphenyl-1,4-phenylene oxide) for gas separation, Journal of Membrane Science 294 (2007) 178.

[31] T.C. Merkel, B.D. Freeman, R.J. Spontak, Z. He, I. Pinnau, P. Meakin, A.J. Hill, Ultrapermeable, reverse-slective nanocomposite membranes, Science 296 (2002) 519.

[32] J.H. Kim, Y.M. Lee, Gas permeation properties of poly(amide-6-b-ethylene oxide)-silica hybrid membranes, Journal of Membrane Science 193 (2001) 209.

[33] X. Hu, H. Cong, Y. Shen, M. Radosz, Nanocomposite membranes for CO_2 separations: silica/brominated poly(phenylene oxide), Industrial and Engineering Chemistry Research 46 (2007) 1547.

[34] A.S. Hay, Poly(2,6-diphenyl-1,4-phenylene oxide), Macromolecules 2 (1969) 107.

[35] F.A. Hamad, G. Chowdhury, T. Matsuura, Sulfonated polyphenylene oxide-polyethersulfone thin-film composite membranes, Journal of Membrane Science 191 (2001) 71.

[36] H. Cong, B. Yu, Aminosilane cross-linked PEG/PEPEG/PPEPG membranes for CO_2/N_2 and CO_2/H_2 separation, Industrial and Engineering Chemistry Research 49 (2010) 9363.

[37] W.J. Koros, A.H. Chan, D.R. Paul, Sorption and transport of various gases in polycarbonate, Journal of Membrane Science 2 (1977) 165.

[38] R.M. Felder, G.S. Huvard, R. Fava, Permeation, Diffusion and Sorption of Gases and Vapors, Academic Press, New York, 1978.

[39] H. Cizchos, T. Saito, L. Smith, Springer Handbook of Materials Measurement Methods, Springer, New York, 2006.

[40] W.H. Lin, R.H. Vora, T.S. Chung, Gas transport properties of 6FDA-Durene/1,4-phenylendiamine (pPDA) copolyimides, Journal of Polymer Science B 38 (2000) 2703.